*Korean J. Chem. Eng.*, 40(6), 1425-1432 (2023)
DOI: 10.1007/s11814-023-1425-z

pISSN: 0256-1115
eISSN: 1975-7220

# Effect of air stone pore size and gas flow rate on the recovery efficiency of paclitaxel from biomass in gas bubble-assisted extraction

**Hyeongjoo Woo and Jin-Hyun Kim†**

Center for Future Sustainable Technology, Department of Chemical Engineering,
Kongju National University, Cheonan 31080, Korea
(*Received 3 November 2022 • Revised 5 January 2023 • Accepted 31 January 2023*)

**Abstract**−The effect of air stone pore size and gas flow rate on the extraction efficiency of gas bubble-assisted extraction to recover paclitaxel derived from *Taxus chinensis* was investigated. The yield of paclitaxel at air stone pore sizes of 10, 30, and 43 μm was 68, 82, and 83% at a gas flow rate of 1.0 L/min, 81, 82, and 85% at a gas flow rate of 1.5 L/min, and 83, 83, and 85% at a gas flow rate of 2.0 L/min, respectively. As the air stone pore size and gas flow rate increased, the yield increased and was significantly improved compared to the 59% yield in the conventional extraction. In addition, as the air stone pore size and gas flow rate increased, the extraction rate constants increased to 1.2302-3.6740 mL/mg·min (10-43 μm, 1.0 L/min), 3.2212-3.9247 mL/mg·min (10-43 μm, 1.5 L/min), and 3.7219-3.9678 mL/mg·min (10-43 μm, 2.0 L/min). The effective diffusion coefficients increased to $3.33928\times10^{-11}-4.16299\times10^{-11}$ $m^2/s$ (10-43 μm, 1.0 L/min), $3.93771\times10^{-11}-4.71392\times10^{-11}$ $m^2/s$ (10-43 μm, 1.5 L/min), and $4.68557\times10^{-11}-4.84878\times10^{-11}$ $m^2/s$ (10-43 μm, 2.0 L/min). While the mass transfer coefficients increased to $3.05840\times10^{-5}-3.71015\times10^{-5}$ m/s (10-43 μm, 1.0 L/min), $3.53749\times10^{-5}-4.13443\times10^{-5}$ m/s (10-43 μm, 1.5 L/min), and $4.11263\times10^{-5}-4.23815\times10^{-5}$ m/s (10-43 μm, 2.0 L/min). A morphological analysis by SEM showed that the bubbles themselves affected cell disruption, and as the air stone pore size and gas flow rate increased, cell disruption accelerated and the recovery efficiency of paclitaxel improved.

Keywords: Paclitaxel, Gas Bubble-Assisted Extraction, Air Stone Pore Size, Gas Flow Rate, Kinetics, Mechanism

## INTRODUCTION

Paclitaxel (Fig. 1) is a diterpenoid natural anticancer substance which was discovered in the epidermis of the Pacific yew *Taxux brevifolia*. It induces apoptosis of cancer cells by inhibiting microtubule depolymerization during cell division. Due to its unique mechanism of action, paclitaxel is a chemotherapeutic drug commonly used in the treatment of ovarian cancer, breast cancer, cervical cancer, lung cancer, and bladder cancer [1-4]. In addition, the demand for paclitaxel is expected to increase because the indications of this drug have expanded (Alzheimer's disease, rheumatoid arthritis) and more treatments have been developed [3-6]. According to data published by the QYR Pharma & Healthcare Research Center in 2018, global paclitaxel production increased from 1,448 kg in 2012 to 2,894 kg in 2018 and is expected to reach 6,195 kg by 2025. Furthermore, the global paclitaxel market size increased from USD 51.2 million in 2012 to USD 90.3 million in 2018 and is expected to grow further to USD 161.7 million by 2025 [7]. The main production methods of paclitaxel include direct extraction from yew trees, semi-synthesis using its precursors, and plant cell culture through callus derived from yew trees. Among them, plant cell culture is advantageous for mass production because it is less influenced by external factors (climate, environment) and can stably and uniformly produce paclitaxel in a bioreactor [2-4].

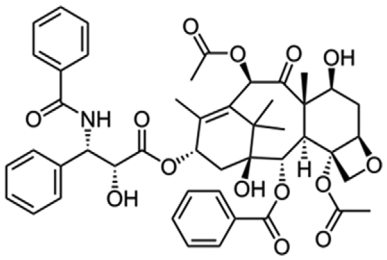

**Fig. 1. The chemical structure of paclitaxel.**

Paclitaxel produced by plant cell culture is a secondary metabolite that is mostly accumulated in plant cells (biomass) [2], and high-purity paclitaxel is obtained through several stages of extraction and purification [4,8,9]. From an economic point of view, it is very important to first recover the paclitaxel accumulated in the biomass in a high yield. Paclitaxel is generally recovered by extraction with organic solvents. Among various organic solvents (acetone, chloroform, ethanol, methanol, methylene chloride, etc.), methanol is known to be the most effective extraction solvent [10]. In addition, the yield of paclitaxel can be increased by optimizing the key process parameters (methanol concentration, biomass/methanol ratio, extraction time, and number of extractions) during extraction [11]. However, conventional solvent extraction requires a large number of organic solvents and a long working time, so the extraction efficiency is low [12,13]. To address this drawback, a process was devel-

†To whom correspondence should be addressed.
E-mail: jinhyun@kongju.ac.kr

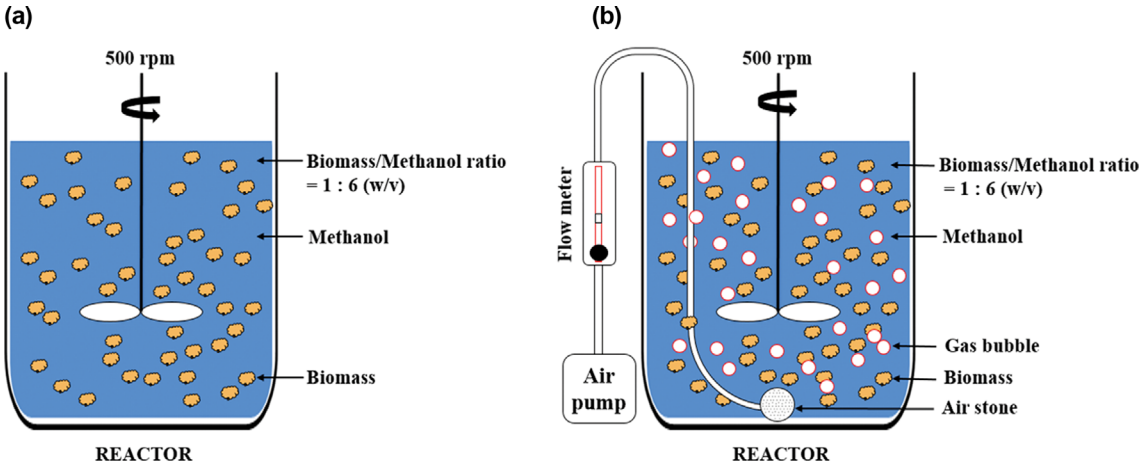


**Fig. 2. Schematic diagrams of paclitaxel extraction from biomass. (a) Conventional extraction; (b) Gas bubble-assisted extraction.**

oped recently to effectively disrupt the biomass by introducing ultrasonic waves to the extraction solution to increase the recovery efficiency of the target material [10,13-19]. This improvement in extraction efficiency is attributed to ultrasonic cavitation, wherein cavitation bubbles collapse during compression and expansion, generating high-speed micro-jets of extraction solution, intense localized heating, and high-pressure shock waves [10,12,19,20]. A recent study confirmed that the roles of cavitation bubbles and gas bubbles were very similar when paclitaxel extraction from biomass was performed by introducing gas bubbles instead of cavitation bubbles [19]. Unlike cavitation bubbles, gas bubbles move without collapsing during their lifetime, so high temperature and high pressure are not generated [19,21,22], and after colliding with the solid (plant cell) surface, they reach the surface of the extraction solution, burst and disappear. For animal cells, it was reported that small bubbles (e.g. <2 mm diameter) cause more damage to cells than large bubbles (e.g. ~10 mm diameter) [23]. On the other hand, in the case of brain neurons, it was found that larger bubble sizes (5-10 nm) cause greater damage to the brain's perineuronal nets [24]. Ultimately, it was found that the effect of bubble size on the degree of cell damage may differ depending on the cell type, and cell damage is directly affected by the gas flow rate [23]. Previous studies have shown that bubble size increases with air flow rate and air stone pore size, as measured photographically in conjunction with image-processing techniques [25]. From an operational point of view, it is much easier to control the air stone pore size than the bubble size in gas bubble-assisted extraction. Considering these characteristics, this study observed for the first time the extraction pattern and extraction mechanism of gas bubble-assisted extraction for recovering plant cell-derived paclitaxel by varying the gas flow rate and air stone pore size. In addition, the effective diffusion coefficient and mass transfer coefficient of paclitaxel were calculated to quantitatively identify the characteristics of gas bubble-assisted extraction.

## MATERIALS AND METHODS

### 1. Plant Materials

Suspension cells derived from *Taxus chinensis* were cultured in modified Gamborg's B5 medium [9] at 24 °C in darkness while agitating (150 rpm). Fresh medium was replaced in the cell culture every two weeks. To extend the production and culture, 1-2% (w/v) of maltose was added on the 7th and 21st days of culture, and 4 μm $AgNO_3$ was added as an elicitor at the initial stage of culture. After cell culture, the plant cells (biomass) were recovered using a decanter (CA150 Clarifying Decanter, GEA Westfalia Separator, Oelde, Germany) and a high-speed centrifuge (BTPX 205GD-35CDEFP, Alfa Laval, Lund, Sweden). The biomass was provided by the Samyang Biopharm Company, Korea.

### 2. Gas Bubble-assisted Extraction

Fig. 2 shows the schematic diagrams of the conventional extraction and the gas bubble-assisted extraction. Conventional extraction was performed once by varying the extraction time (1, 2, 4, 6, 8, 10, and 12 min) at a biomass/methanol ratio of 1 : 6 (w/v), room temperature, and an agitation speed of 500 rpm [10]. For gas bubble-assisted extraction, the gas flow rate (1.0, 1.5, and 2.0 L/min) was varied with an air pump (AP-1802, ZEDEE, China) and a flow meter (RMA-26-SSV, Dwyer, U.S.A). The gas bubble sizes were varied by an air stone (pore size: 10, 30, and 43 mm). Other extraction conditions were set the same as those of the conventional extraction. The reactor size and working volume were 100 mL and 30 mL, respectively. After extraction, the paclitaxel extraction filtrate was recovered by filtration (5A 185 mm, ADVANTEC, Japan) under reduced pressure (A-3S, EYELA, Japan), concentrated using a concentrator (CCA-1100, EYELA, Japan), and then vacuum dried at 40 °C for 24 hr (SH-VDO-30NG, SH SCIENTIFIC, Korea). The paclitaxel content in the dried extract was analyzed by HPLC. The quantity of paclitaxel in the biomass was obtained through multiple extractions, and the yield of paclitaxel was calculated with Eq. (1) [12].

$$\text{Yield}\ (\%) = \frac{\text{Quantity of pure paclitaxel in crude paclitaxel}}{\text{Quantity of pure paclitaxel in biomass}} \times 100 \quad (1)$$

### 3. Analysis of Paclitaxel

The content of paclitaxel was analyzed using an HPLC system (SCL-10AVP, Shimadzu, Japan) equipped with a Capcell Pak $C_{18}$ col-

umn (250×4.6 mm, Shiseido, Japan). For the mobile phase, an acetonitrile-distilled water mixed solution (35/65-65/35, v/v, gradient mode) was made to flow at a flow rate of 1.0 mL/min for 40 min. The amount of sample injected was 20 μL and it was detected by UV at 227 nm [5]. Authentic paclitaxel (purity: 95%) as a standard was purchased from Sigma-Aldrich.

**4. SEM Analysis**

The biomass surface change before and after extraction was examined using a scanning electron microscope (MIRA LMH; Tescan, Czech Republic). The sample used for analysis was about 1 mg and the images were obtained with a magnification of 3,000 times at an acceleration voltage of 10 kV [5].

**5. Kinetic Models**

For the kinetic analysis of the extraction, extraction data were applied to a pseudo-first-order model, a pseudo-second-order model, and an intraparticle diffusion model [12,26-28]. The effective diffusion coefficient and mass transfer coefficient were calculated using a model formula based on Fick's second law [12,29-31]. Since Biot numbers are effective in the extraction process, the relative magnitude of the internal and external resistance of the biomass during mass transfer was calculated using Biot numbers [31,32]. The model equations used for the kinetic study are arranged in Table 1. Each parameter of the model equation was calculated as a linear equation based on linear regression analysis in Sigmaplot 10.0 (Systat software Inc., USA). The validity of the model was evaluated by determination coefficient ($r^2$) and root mean squared deviation (RMSD). RMSD is expressed as Eq. (2).

$$\mathrm{RMSD}=\sqrt{\frac{1}{n}\sum_{i=1}^{n}(\mathrm{experimental}-\mathrm{calculated})^2} \quad (2)$$

where n is the number of experiments.

## RESULTS AND DISCUSSION

**1. Effect of Air Stone Pore Size and Gas Flow Rate in the Gas Bubble-assisted Extraction**

Fig. 3 shows the yield of paclitaxel in the conventional extraction and gas bubble-assisted extraction. In the case of the conventional extraction, the yield of paclitaxel was 59% at 10 min of extraction, and then the reaction reached an equilibrium. Whereas for gas bubble-assisted extraction, the yield of paclitaxel at air stone pore sizes 10, 30, and 43 μm was 68, 82, and 83% at a gas flow rate of 1.0 L/min, 81, 82, and 85% at 1.5 L/min, and 83, 83, and 85% at 2.0 L/min, respectively. As the gas flow rate and air stone pore size increased, the yield of paclitaxel increased, and there was no significant difference in the yield at gas flow rates higher than 1.5 L/min and air stone pore sizes larger than 30 μm. In addition, as the extraction time increased, the yield of paclitaxel also increased, and the extraction nearly reached equilibrium after 10 min. Such results are similar to those found in cavitation bubble-assisted extraction for the recovery of biomass-derived paclitaxel [19]. Thus, the roles of gas bubbles and cavitation bubbles in the extraction process are similar, and the bubbles themselves act as a key factor in improving extraction efficiency.

**Table 1. Equations used for parameter estimation in this study**

| Equation | Parameter | Ref. |
|---|---|---|
| First-order model<br>$\ln(C_e-C_t)=\ln C_e-k_1 t$ | $C_t$ (mg/mL): conc. of paclitaxel at time t<br>$C_e$ (mg/mL): conc. of extracted paclitaxel at equilibrium<br>$k_1$ ($min^{-1}$): pseudo-first-order rate constant | [5,11] |
| Second-order model<br>$\frac{t}{C_t}=\frac{1}{k_2 C_e^2}+\frac{t}{C_e}$<br>$h=k_2 C_e^2$ | $k_2$ (mL/mg·min): pseudo-second-order rate constant<br>h (mg/mL·min): initial extraction rate | [11,24] |
| Intraparticle diffusion model<br>$q_t=k_p t^{1/2}$ | $q_t$: yield of paclitaxel extracted in the suspension at time t<br>kp (mg/g·$min^{1/2}$): intraparticle diffusion rate constant | [11,26] |
| Fick's law<br>$\ln\left(\frac{Y_s}{Y_s-Y_t}\right)=\ln\frac{\pi^2}{6}+\frac{D_e\pi^2 t}{R^2}$ | $Y_s$: total paclitaxel yield at saturation<br>$Y_t$: total paclitaxel yield at time t<br>$D_e$ ($m^2$/s): effective diffusion coefficient<br>R: cell radius (average radius: $27.5\times10^{-6}$ m) | [27-29] |
| $\ln\frac{C_s}{C_s-C_t}=\frac{K_T A}{V_s}t$<br>$A=\frac{3m_{plant}}{\rho_{r_p}}$ | $C_s$ (mg/mL): saturation concentration of paclitaxel<br>$C_t$ (mg/mL): concentration of paclitaxel at time t<br>A ($m^2$): total surface area of the particles (cells)<br>$m_{plant}$ (kg): cell weight introduced in the extractor<br>$\rho$: cell wet density (1,071.43 kg/$m^3$)<br>$r_p$: cell size (average radius: $27.5\times10^{-6}$ m)<br>$V_s$ ($m^3$): volume of solution<br>$K_T$ (m/s): mass transfer coefficient | [11,29] |
| $Bi=\frac{r_p K_T}{D_e}$ | Bi: mass transfer Biot number | [11,29,30] |

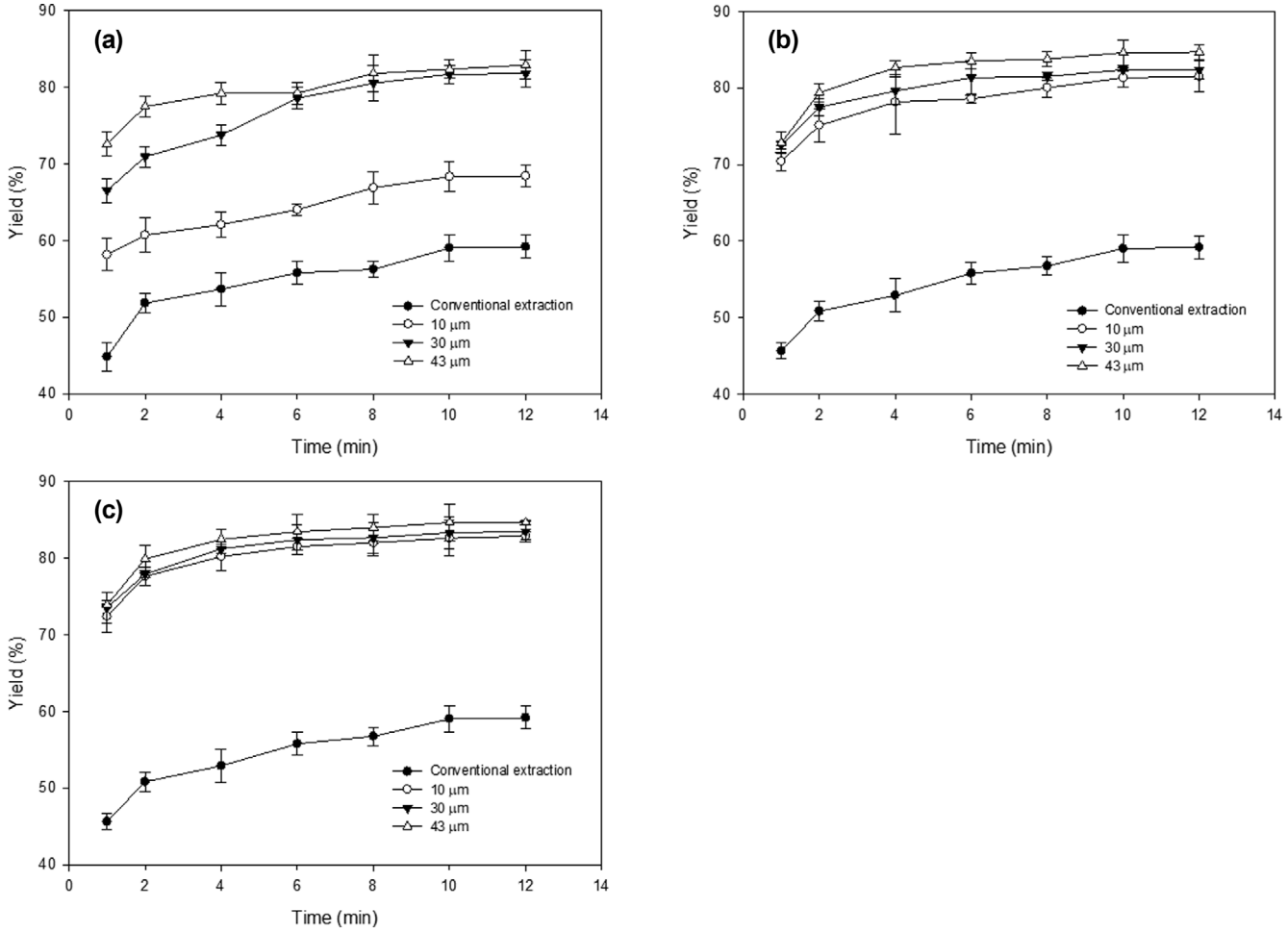


**Fig. 3. Effect of air stone pore size on the yield of paclitaxel from biomass at different gas flow rates in conventional extraction and bubble-assisted extraction. (a) Gas flow rate of 1.0 L/min; (b) Gas flow rate of 1.5 L/min; (c) Gas flow rate of 2.0 L/min.**

The surface of the biomass before and after extraction was observed through SEM analysis. Before extraction, the biomass surface was very smooth without cracks (Fig. 4(a)). After conventional extraction, the biomass surface was slightly wrinkled and crushed (Fig. 4(b)). On the other hand, after gas bubble-assisted extraction, the biomass surface was much rougher, more shrunken and fractured compared to the biomass after conventional extraction (Fig. 4(c)-Fig. 4(k)). This phenomenon became more pronounced as the gas flow rate and air stone pore size increased. The larger the gas flow rate and air stone pore size, the stronger the impact on the biomass surface, allowing for paclitaxel to be more easily extracted from the biomass. However, there was no significant difference in biomass surface change at gas flow rates higher than 1.5 L/min and air stone pore sizes larger than 30 μm. It is known that the effect of bubble size on the magnitude of cell damage differs depending on the type of cell [23]. The results of this study show that plant cells were strongly impacted as the bubble size increased. This result is similar to that of a study that found that larger bubble sizes (5-10 nm) did greater damage to the cells of brain neurons [24]. The effect of gas flow rate and air stone pore size on the cell wall of plant cells in gas bubble-assisted extraction is schematically shown in Fig. 5. It shows that the larger the gas flow rate and air stone pore size, the greater the impact on the cell wall (cellulose), thereby breaking the glycosidic bond, and facilitating cell disruption. This was also consistent with the SEM analysis results of the biomass surface after extraction according to the gas flow rate and air stone pore size.

**2. Kinetic Studies**

The $r^2$ and RMSD were examined by applying the data obtained from the gas bubble-assisted extraction to kinetic models (first-order model, second-order model) and the second-order model was found to be the best fit. After plotting as $t/C_t$ versus t using a linearized second-order model, the extraction rate constant ($k_2$), equilibrium concentration of paclitaxel ($C_e$), and initial extraction rate (h) were obtained through the slope and y-intercept and are shown in Table 2. In conventional extraction, the $C_e$ was 0.5828 mg/mL, the $k_2$ was 0.6853 mL/mg·min, and the h was 0.2328 mg/mL·min at equilibrium. Whereas in the gas bubble-assisted extraction, $C_e$ (0.6795-0.8326 mg/mL at 10-43 μm and 1.0 L/min, 0.8142-0.8565 at 10-43 μm and 1.5 L/min, and 0.8361-0.8581 at 10-43 μm and 2.0 L/min), $k_2$ (1.2302-3.6740 mL/mg min at 10-43 μm and 1.0 L/min, 3.2212-3.9247 mL/mg min at 10-43 μm and 1.5 L/min, and 3.7219-3.9678 mL/min at 10-43 μm and 2.0 L/min), and h (0.5680-2.5472 mg/mL min at 10-43 μm and 1.0 L/min, 2.1354-2.8788 mg/mL·

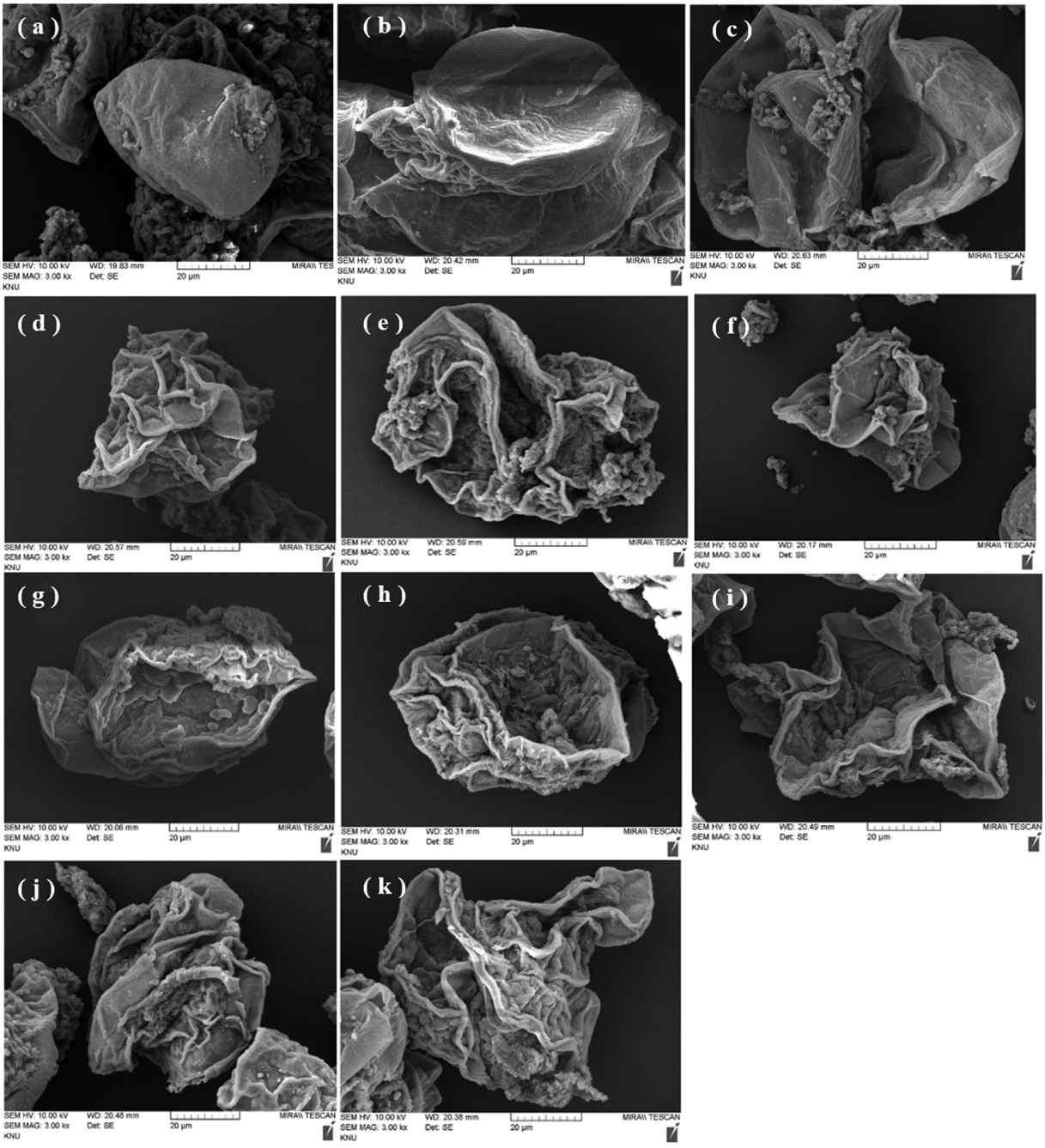


**Fig. 4. SEM images of biomass samples dried by extraction. (a) Before extraction; (b) After conventional extraction; (c) After gas bubble-assisted extraction (1.0 L/min, 10 μm); (d) After gas bubble-assisted extraction (1.0 L/min, 30 μm); (e) After gas bubble-assisted extraction (1.0 L/min, 43 μm); (f) After gas bubble-assisted extraction (1.5 L/min, 10 μm); (g) After gas bubble-assisted extraction (1.5 L/min, 30 μm); (h) After gas bubble-assisted extraction (1.5 L/min, 43 μm); (i) After gas bubble-assisted extraction (2.0 L/min, 10 μm); (j) After gas bubble-assisted extraction (2.0 L/min, 30 μm); (k) After gas bubble-assisted extraction (2.0 L/min, 43 μm).**

min at 10-43 μm and 1.5 L/min, and 2.6016-2.9219 mg/mL·min at 10-43 μm and 2.0 L/min) all increased. In all conditions, $C_e$, $k_2$, and h showed higher values compared to those of the conventional extraction. These results are similar to those in ultrasonic cavitation bubble-assisted extraction for the recovery of paclitaxel from *Taxus chinensis* [19]. This means that the paclitaxel accumulated in the biomass diffuses rapidly into the extraction solution, thereby improving the extraction efficiency. There was no significant difference in $C_e$, $k_2$, and h values at gas flow rates higher than 1.5 L/min and air stone pore sizes larger than 30 μm, which was similar to the yield pattern of paclitaxel. As a result, gas bubble-assisted extraction significantly improved the recovery efficiency of biomass-derived paclitaxel compared to that of the conventional extraction. The second-order model had high $r^2$ values (>0.9984) and small RMSD values (<0.02798) in all conditions, so it was considered a good fit.

**Table 2. Parameters of pseudo-second-order model for gas bubble-assisted extraction of paclitaxel from biomass**

| Gas flow rate (L/min) | Pore diameter (μm) | $C_e$ (mg/mL) | $k_2$ (mL/mg·min) | h (mg/mL·min) | $r^2$ (-) | RMSD (-) |
|---|---|---|---|---|---|---|
| - | Conventional extraction | 0.5828 | 0.6853 | 0.2328 | 0.9998 | 0.01177 |
| 1.0 | 10 | 0.6795 | 1.2302 | 0.5680 | 0.9984 | 0.02344 |
| | 30 | 0.8325 | 1.6579 | 1.1492 | 0.9987 | 0.02798 |
| | 43 | 0.8326 | 3.6740 | 2.5472 | 0.9995 | 0.01032 |
| 1.5 | 10 | 0.8142 | 3.2212 | 2.1354 | 0.9999 | 0.00487 |
| | 30 | 0.8310 | 3.8685 | 2.6713 | 0.9999 | 0.00319 |
| | 43 | 0.8565 | 3.9247 | 2.8788 | 0.9999 | 0.00534 |
| 2.0 | 10 | 0.8361 | 3.7219 | 2.6016 | 0.9999 | 0.00157 |
| | 30 | 0.8459 | 3.7247 | 2.6651 | 0.9999 | 0.00439 |
| | 43 | 0.8581 | 3.9678 | 2.9219 | 0.9999 | 0.00241 |

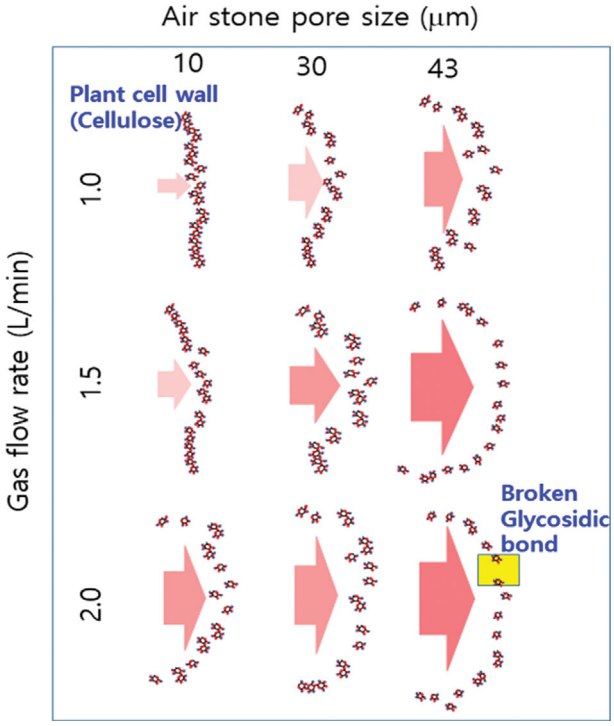


**Fig. 5. Hypothetical mechanisms proposed to explain the impact of gas flow rate and air stone pore size on the plant cell wall (cellulose) in gas bubble-assisted extraction. Arrow heads illustrate the stream of gas bubbles and their widths represent shock strength.**

The extraction mechanism was analyzed by applying the intraparticle diffusion model, which is generally used in the adsorption process, to the extraction process. The data obtained from the gas bubble-assisted extraction were applied to the intraparticle diffusion model and plotted as $q_t$ versus $t^{1/2}$ (Fig. 6). The intraparticle diffusion model has multiple linear characteristics and can be analyzed by dividing it into three steps [12,28]. This means that the extraction proceeds in three stages. Stage I is a washing step, in which paclitaxel is dissolved in methanol on the surface of the biomass. Stage II is a diffusion step, in which paclitaxel moves from inside of the biomass to the surface. Stage III is an equilibrium step, in which extraction reaches equilibrium [5]. In the case of the conventional extraction, the washing step and the diffusion step are clearly divided, and the extraction proceeds step by step. On the other hand, in the case of gas bubble-assisted extraction with a gas flow rate of 1.0 L/min, as the air stone pore size increases, the boundary between the washing step and the diffusion step becomes more and more vague, and washing and diffusion proceed almost simultaneously. However, at gas flow rates higher than 1.5 L/min, washing and diffusion are performed almost simultaneously regardless of the air stone pore size. This trend is also seen in ultrasonic cavitation bubble-assisted extraction [19], which means that the roles of gas bubbles and ultrasonic cavitation bubbles in the extraction process are similar. In Fig. 6, diffusion is not the only rate-limiting step since the straight line of the diffusion step does not pass through the origin. However, since the extraction rate constant was smaller in the diffusion step than in the washing step, diffusion greatly affected the rate-limiting step.

## 3. Calculation of Effective Diffusion Coefficient and Mass Transfer Coefficient

The effective diffusion coefficient ($D_e$), mass transfer coefficient ($K_T$), and Biot number ($B_i$) were calculated in conventional extraction and the gas bubble-assisted extraction, and they are presented in Table 3. $D_e$ was $2.92398\times10^{-11}$ $m^2/s$ in the conventional extraction, while in the gas-bubble-assisted extraction the values were $3.33928\times10^{-11}$–$4.16299\times10^{-11}$ $m^2/s$ (10-43 μm, 1.0 L/min), $3.93771\times10^{-11}$–$4.71392\times10^{-11}$ $m^2/s$ (10-43 μm, 1.5 L/min), and $4.68557\times10^{-11}$–$4.84878\times10^{-11}$ $m^2/s$ (10-43 μm, 2.0 L/min). These values showed a 14-66% increase compared to the conventional extraction. In the conventional extraction, the $K_T$ was $2.75786\times10^{-5}$ m/s, and in the gas bubble-assisted extraction the values were $3.05840\times10^{-5}$–$3.71015\times10^{-5}$ m/s (10-43 μm, 1.0 L/min), $3.53749\times10^{-5}$–$4.13443\times10^{-5}$ m/s (10-43 μm, 1.5 L/min), and $4.11263\times10^{-5}$–$4.23815\times10^{-5}$ m/s (10-43 μm, 2.0 L/min). These values had a 10-54% increase compared to the conventional extraction. As the gas flow rate and air stone pore size increased, both the effective diffusion coefficient and the mass transfer coefficient increased, and the mass transfer coefficient increased more significantly than the effective diffusion coefficient. This trend is consistent with the results of previous studies

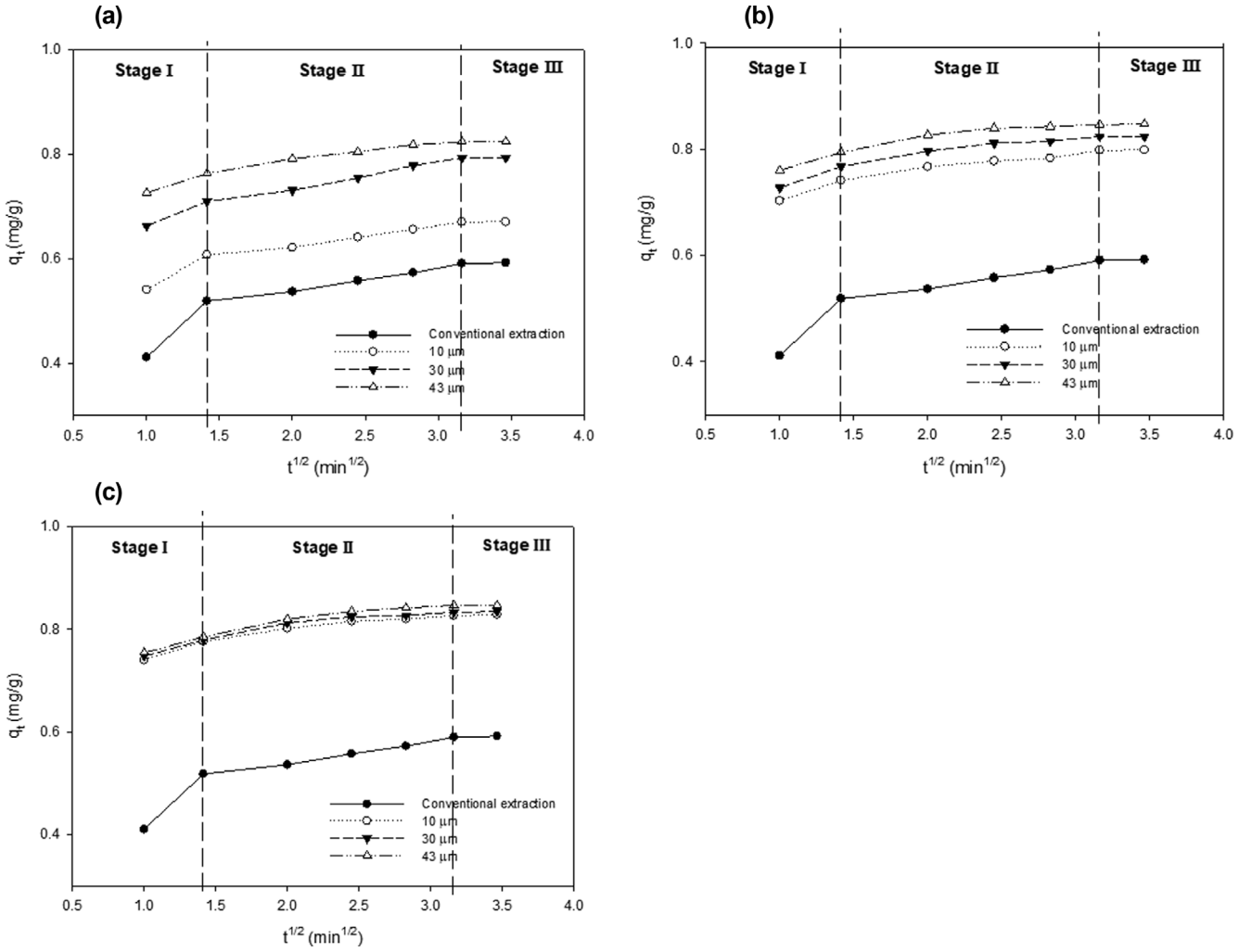


**Fig. 6. Intraparticle diffusion plot for gas bubble-assisted extraction of paclitaxel from biomass. (a) Gas flow rate of 1.0 L/min; (b) Gas flow rate of 1.5 L/min; (c) Gas flow rate of 2.0 L/min.**

**Table 3. Values of the effective diffusion coefficient ($D_e$), the mass transfer coefficient ($K_T$), and Biot number ($B_i$) obtained for gas bubble-assisted extraction of paclitaxel from biomass**

| Gas flow rate (L/min) | Pore diameter (μm) | $D_e \times 10^{13}$ ($m^2/s$) | $K_T \times 10^7$ (m/s) | $B_i$ (-) |
|---|---|---|---|---|
| - | Conventional extraction | 2.92398 | 2.75786 | 25.93767 |
| 1.0 | 10 | 3.33928 | 3.05840 | 25.18684 |
| | 30 | 3.65421 | 3.31945 | 24.98078 |
| | 43 | 4.16299 | 3.71015 | 24.50860 |
| 1.5 | 10 | 3.93771 | 3.53749 | 24.70491 |
| | 30 | 4.65185 | 4.08611 | 24.15556 |
| | 43 | 4.71392 | 4.13443 | 24.11942 |
| 2.0 | 10 | 4.68557 | 4.11263 | 24.13739 |
| | 30 | 4.83115 | 4.22459 | 24.04734 |
| | 43 | 4.84878 | 4.23815 | 24.03681 |

on the effect of gas flow rate on the effective diffusion coefficient and the mass transfer coefficient [19]. Also, similar to the yield pattern of paclitaxel, there was no significant difference in $D_e$ and $K_T$ values at gas flow rates higher than 1.5 L/min and air stone pore sizes larger than 30 μm. A high Biot number (>20) indicates that the external resistance for mass transfer is negligible, which means

mixing between the solvent and the solute is efficiently executed [5,12]. Therefore, it was confirmed that internal transfer was a rate-limiting step.

## CONCLUSIONS

The effect of gas flow rate and air stone pore size on the gas bubble-assisted extraction of biomass-derived paclitaxel was investigated, and the extraction mechanism was analyzed through a kinetic study. The yield of paclitaxel at air stone pore sizes of 10, 30, and 43 μm was 68, 82, and 83% at gas flow rates of 1.0 L/min, 81, 82, and 85% at 1.5 L/min, and 83, 83, and 85% at 2.0 L/min, respectively. As the gas flow rate and air stone pore size increased, the yield of paclitaxel increased. At gas flow rate higher than 1.5 L/min and air stone pore size larger than 30 μm, the yield increase was not significant. In addition, the SEM analysis showed that the biomass surface became rougher, more contracted and destroyed as the gas flow rate and air stone pore size increased. The pseudo-second-order kinetic model was well fit to the extraction data with high $r^2$ values (>0.9984) and small RMSD values (<0.02798). In addition, washing and diffusion were performed almost simultaneously according to the intraparticle diffusion model, and intraparticle diffusion played a dominant role in the extraction rate. As the gas flow rate and air stone pore size increasd, the rate constant (1.2302-3.6184 mL/mg min at 10-43 μm and 1.0 L/min, 3.212-3.9247 mL/mg min at 10-43 μm and 1.5 L/min, 3.7219-3.9678 mL/mg min at 10-43 μm and 2.0 L/min), the effective diffusion coefficient ($3.33928\times10^{-11}$–$4.16299\times10^{-11}$ $m^2/s$ at 10-43 μm and 1.0 L/min, $3.93771\times10^{-11}$–$4.71392\times10^{-11}$ at 10-43 μm and 1.5 L/min, $4.68557\times10^{-11}$–$4.84878\times10^{-11}$ at 10-43 μm and 2.0 L/min), and the mass transfer coefficient ($3.05840\times10^{-5}$–$3.71015\times10^{-5}$ m/s at 10-43 μm and 1.0 L/min, $3.53749\times10^{-5}$–$4.13443\times10^{-5}$ m/s at 10-43 μm and 1.5 L/min, $4.11263\times10^{-5}$–$4.23815\times10^{-5}$ m/s at 10-43 μm and 2.0 L/min) increased. Also, due to a high Biot number (>20), the external resistance for mass transfer during the extraction process was ignored and the internal transfer was regarded as the rate-limiting step.

## ACKNOWLEDGEMENTS

This work was supported by the National Research Foundation of Korea (NRF) grant funded by the Government of Korea (MSIT) (Grant Number: 2021R1A2C1003186).

## REFERENCES

1. L. Zhu and L. Chen, *Cell. Mol. Biol. Lett.*, **24**, 40 (2019).
2. H. S. Min, H. G. Kim and J. H. Kim, *Korean J. Chem. Eng.*, **39**, 398 (2022).
3. Y. S. Jang and J. H. Kim, *Biotechnol. Bioprocess Eng.*, **24**, 529 (2019).
4. J. H. Kim, *Korean J. Biotechnol. Bioeng.*, **21**, 1 (2006).
5. H. S. Min and J. H. Kim, *Biotechnol. Bioprocess Eng.*, **27**, 111 (2022).
6. M. Ghorbani, F. Pourjafar, M. Saffari and Y. Asgari, *Meta Gene*, **26**, 100800 (2020).
7. H. S. Min, M.S. Thesis, Kongju National University, Cheonan, Korea (2022).
8. C. G. Lee and J. H. Kim, *Process Biochem.*, **51**, 1738 (2016).
9. S. H. Pyo, H. B. Park, B. K. Song, B. H. Han and J. H. Kim, *Process Biochem.*, **39**, 316 (2004).
10. J. H. Kim, *Korean Chem. Eng. Res.*, **58**, 273 (2020).
11. J. H. Kim and S. S. Hong, *Korean J. Biotechnol. Bioeng.*, **15**, 346 (2000).
12. K. W. Yoo and J. H. Kim, *Biotechnol. Bioprocess Eng.*, **23**, 532 (2018).
13. S. H. Lee and J. H. Kim, *Process Biochem.*, **76**, 187 (2019).
14. W. Tang, B. Wang, M. Wang and M. Wang, *J. Appl. Res. Med. Aromat. Plants*, **25**, 100331 (2021).
15. R. Upadhyay, G. Nachiappan and H. N. Mishra, *Food Sci. Biotechnol.*, **24**, 1951 (2015).
16. G. Wang, Q. Cui, L. J. Yin, Y. Li, M. Z. Gao, Y. Meng, J. Li and S. D. Zhang, *Sep. Purif. Technol.*, **244**, 115805 (2020).
17. T. Wang, N. Guo, S. X. Wang, P. Kou, C. J. Zhao and Y. J. Fu, *Food Bioprod. Process*, **108**, 69 (2018).
18. G. S. Ha and J. H. Kim, *Process Biochem.*, **51**, 1664 (2016).
19. H. G. Kim and J. H. Kim, *Biotechnol. Bioprocess Eng.*, **27**, 668 (2022).
20. D. Panda and S. Manickam, *Appl. Sci.*, **9**, 766 (2019).
21. H. J. Kang and J. H. Kim, *Process Biochem.*, **99**, 316 (2020).
22. K. Wohlgemuth, A. Kordylla, F. Ruether and G. Schembecker, *Chem. Eng. Sci.*, **64**, 4155 (2009).
23. Y. Chisti, *Trends Biotechnol.*, **18**, 420 (2000).
24. Y. T. Wu and A. Adnan, *Sci. Rep.*, **7**, 5323 (2017).
25. S. Chen, M. B. Timmons, D. J. Aneshansley and J. J. Bisogni Jr., *Aquacult. Eng.*, **11**, 267 (1992).
26. Y. S. Ho, H. A. Harouna-Oumarou, H. Fauduet and C. Porte, *Sep. Purif. Technol.*, **45**, 169 (2005).
27. M. G. Shashidhar, P. Giridhar and B. Manohar, *Biochem. Eng. J.*, **121**, 88 (2017).
28. A. Pholosi, E. B. Naidoo and A. E. Ofomaja, *S. Afr. J. Chem. Eng.*, **32**, 39 (2020).
29. R. Y. Krishnan and K. S. Rajan, *Sep. Purif. Technol.*, **157**, 169 (2016).
30. R. Y. Krishnan, M. N. Chandran, V. Vadivel and K. S. Rajan, *Sep. Purif. Technol.*, **170**, 224 (2016).
31. L. Rakotondramasy-Rabesiaka, J. L. Havet, C. Porte and H. Fauduet, *Sep. Purif. Technol.*, **76**, 126 (2010).
32. P. C. Setford, D. W. Jeffery, P. R. Grbin and R. A. Muhlack, *Molecules*, **24**, 73 (2019).